Preparation, Characterization, and Properties of Sodium Montmorillonite Clay/Poly(styrene–butadiene–styrene) Containing Quaternary Ammonium Cations and Photoinitiator Nanocomposites via Ultraviolet Exposure

Guoliang Wu, Yanyan Xie, Encai Ou, Lala Zhang, Yuanqin Xiong, Weijian Xu

Institute of Polymer Science and Engineering, College of Chemistry and Chemical Engineering, Hunan University, Changsha 410082, China

Received 24 February 2010; accepted 7 April 2010
DOI 10.1002/app.32576
Published online 3 June 2010 in Wiley InterScience (www.interscience.wiley.com).

ABSTRACT: A functionalized graft copolymer {poly(styrene–butadiene–styrene) (SBS)-*g*-4-benzoyl-*N*,*N*-dimethyl-*N*-[2-(2-methyl-1-oxo-2-propenyloxy)ethyl]benzenemethanaminium bromide (4-BBPDMAEMA)}, containing a photoinitiator, quaternary ammonium cations, and many C=C double bonds, was synthesized to modify clays, such as Na^+–montmorillonite (MMT) clay, for the preparation of organic–inorganic nanocomposite resins via radical photoinduced crosslinking polymerization. The structure of SBS-*g*-4-BBPDMAEMA was characterized by Fourier transform infrared and ^{1}H-NMR spectroscopy. The corresponding SBS-*g*-4-BBPDMAEMA was found to have two functions: the capability to ionically exchange with sodium ions in the silicate gallery and the capability to synthesize exfoliated SBS/MMT nanocomposites by the UV crosslinking of intercalation polymerization. The results from the X-ray diffraction primarily reveal that the clay platelets should have been exfoliated or completely disordered. However, the results from transmission electron microcopy confirmed that a mixture of partially exfoliated and intercalated structures presented in the nanocomposites. Dynamic mechanical thermal analysis testing indicated that the glass-transition temperature of the polybutadiene phase and polystyrene phase moved to a lower temperature. Data of thermogravimetric analysis and testing of the mechanical properties showed that the thermal stability and mechanical properties of SBS-*g*-4-BBPDMAEMA could be regulated by the crosslinking and content of MMT. © 2010 Wiley Periodicals, Inc. J Appl Polym Sci 118: 1675–1682, 2010

Key words: block copolymers; crosslinking; nanocomposites; photopolymerization; polymer synthesis and characterization

INTRODUCTION

For the past 20 years, there has been increased attention paid to the synthesis of nanocomposites based on either intercalated or exfoliated clay dispersed into various matrix polymers.[1–6] Compared with conventional composites, nanocomposites often exhibit a great improvement in the mechanical properties,[7–17] gas permeability,[18–23] heat resistance,[24] and fire-retardance[25–28] properties at very low clay contents of generally less than 5 wt %. However, exfoliated nanocomposites frequently exhibit more unexpected properties synergistically derived from the two components than do intercalated nanocomposites; to date, there have been many reports of intercalated nanocomposite structures within a block copolymer matrix[29–32] because the formation of exfoliated nanocomposites is different because of the unfavorable interactions between the intrinsically hydrophilic clay and the hydrophobic matrix polymer chains.

Poly(styrene–butadiene–styrene) (SBS) has been widely used as a thermoplastic elastomer. Laus et al.[33] prepared intercalated SBS/clay nanocomposites by melt blending for the first time, and the nanocomposites exhibited enhanced moduli. Chen and Feng[34] prepared SBS/montmorillonite (MMT) nanocomposites with excellent mechanical properties via the *in situ* polymerization/melt compounding combination technique. Liao et al.[35] reported intercalated SBS/clay nanocomposites prepared by a solution approach, indicating that the nanocomposites exhibited increased thermal and mechanical properties. Recently, Zhang et al.[36] prepared intercalated SBS/clay nanocomposites that showed improved radiation stability in comparison with pure SBS. Ha et al.[37] created orientationally ordered hierarchical nanocomposites by the preferential insertion of individual polymer-covered clay layers into block copolymer microdomains. Liao et al.[38] prepared intercalated star-shaped and linear SBS/organophilic montmorillonite (OMMT) clay

Correspondence to: W. Xu (weijianxu_59@163.com).
Contract grant sponsor: Baling Petrochemical Co., Ltd., China.

nanocomposites by a solution approach and showed that the mechanical strength of the nanocomposites with the star-shaped SBS/OMMT were significantly increased. The addition of OMMT also provided increases in the elongation, dynamic storage modulus (E'), dynamic loss modulus (E''), and thermal stability of the nanocomposites. Chang et al.[39] synthesized comb-branched copolymers consisting of a hydrophobic polystyrene-*b*-poly(ethylene/butylene)-*b*-polystyrene backbone and multiple pendants of polyoxyalkylene quaternary ammonium salts to intercalate with layered silicates. They found that the emulsion intercalation was a viable process for tailoring various hydrophobic organic/silicate hybrids. However, completely exfoliated SBS/clay nanocomposites have scarcely been reported. To date, the preparation of an exfoliated nanocomposite structure within a block copolymer matrix has been difficult work. Although methods of organically functionalizing the surfaces of the clay with the inherent negative surface charges on the clay layers have been successfully developed, it is difficult to prepare nanocomposites with exfoliated structures because of the very strong electrostatic interactions between the silicate layers.

From the previous studies, we know that when polymerization occurs between the layers of MMT, one can prepare exfoliated nanocomposites. Therefore, in this study, a functionalized graft copolymer, SBS-*g*-4-benzoyl-*N*,*N*-dimethyl-*N*-[2-(2-methyl-1-oxo-2-propenyloxy)ethyl]benzenemethanaminium bromide (4-BBPDMAEMA), containing a photoinitiator, quaternary ammonium cations, and many C=C double bonds, was synthesized to modify MMT for the preparation of organic/inorganic nanocomposites resins via a radical photoinduced crosslinking polymerization. The corresponding SBS-*g*-4-BBPDMAEMA was found to have two functions:

1. The ability to ionically exchange with sodium ions in the silicate gallery because of the presence of multiple ammonium salts (—$NH_3^+Br^-$) as the grafting pendants. Then, the grafted copolymer containing photoinitiator and many C=C bonds also entered into the silicate gallery
2. The ability to synthesize an exfoliated SBS/MMT nanocomposites by the UV crosslinking of intercalation polymerization.

The structure of the SBS/MMT nanocomposites was studied by X-ray diffraction (XRD) and transmission electron microscopy (TEM). Furthermore, the glass-transition temperatures (T_g), thermal stability, and mechanical properties of the crosslinked nanocomposites were studied in detail.

EXPERIMENTAL

Materials

The triblock polymer SBS was provided by Baling Oil Chemical Industry Co. (Yueyang, China) and was used without further purification. The SBS (YH-792) was comprised of 40 wt % polystyrene (PS) and sold stabilized with 0.14 wt % 2,6-di-*tert*-butyl-4-methylphenol antioxidant. Gel permeation chromatography analysis of the SBS in tetrahydrofuran gave number-average molecular weight fractions of 22,800 (40%) and 68,400 (60%) with a polydispersity of 1.15. Sodium montmorillonite (Na^+–MMT), with a 1.10 mequiv/g cationic exchange capacity (CEC), was obtained from the local supermarket. 4-Bromomethyl benzophenone (4-BBP) and dimethyl amino ethyl methacrylate were purchased from Aldrich (Beijing, China) and were used directly without further purification. Benzoyl peroxide was recrystallized from chloroform and dried in a desiccator. Toluene and other solvents were all analytically pure and were used as received.

Synthesis of 4-BBPDMAEMA and SBS-*g*-4-BBPDMAEMA as intercalating agents

4-BBPDMAEMA was synthesized by the method in ref. 40.

^{1}H-NMR ($CDCl_3$, δ): 1.972 (3, CH_3), 3.475 (6, CH_3), 4.272 (2, CH_2), 4.749 (2, CH_2), 5.439 (2, CH_2), 5.954 (1, CH), 6.141 (1, H), 7.480 (2, ArH), 7.605 (1, ArH), 7.767 (2, ArH), 7.824 (2, ArH), 7.937 (2, ArH). Fourier transform infrared (FTIR) spectroscopy (KBr, cm^{-1}): 1716 (C=O); 1657 1660 (—CH=C (CH_3)—); 1180 (C—O).

The grafting reaction of 4-BBPDMAEMA on SBS was carried out in toluene solvent in a 100-mL, four-necked glass flask equipped with a stirrer, thermometer, condenser, and nitrogen inlet. A brief description of the procedure is as follows: 2 g of SBS and 0.4 g of 4-BBPDMAEMA were dissolved in 20 mL of toluene, and then, a certain amount of the benzoyl peroxide initiator was added dropwise. The reaction solution was stirred for 8 h at 60°C. After the reaction finished, the polymer was coagulated in methanol. Finally, the residual 4-BBP was extracted in a Soxhlet extractor (Changsha, China) with methanol for 24 h, and the grafted SBS (SBS-*g*-4-BBPDMAEMA) was obtained after vacuum drying. The theoretical molecular structure of the resulting SBS-*g*-4-BBPDMAEMA is shown in Scheme 1.

Preparation of the SBS/MMT nanocomposites

Scheme 2 illustrates our synthesis route for the preparation of the SBS/MMT nanocomposites. The

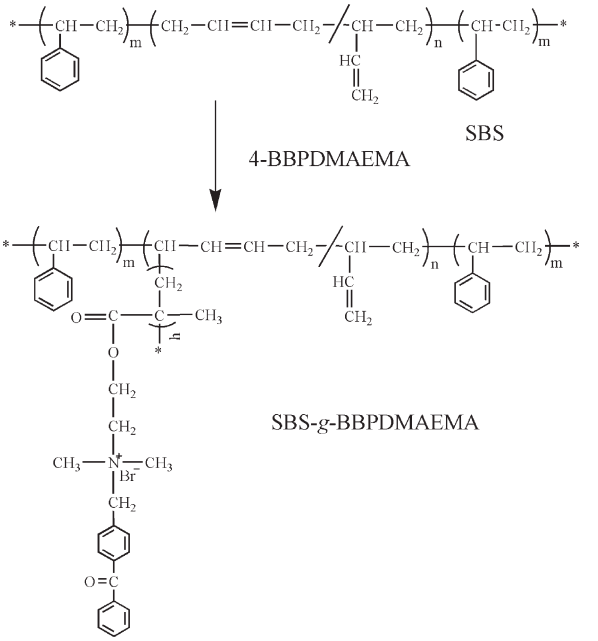

Scheme 1 Synthesis process of SBS-*g*-4-BBPDMAEMA.

SBS/MMT nanocomposites were prepared by solution processing as follows. Na^+–MMT (3.0 g) was dispersed in 20 mL of toluene and stirred vigorously at 80°C for 3 h. The slurry was added to SBS-*g*-4-BBPDMAEMA, which had been previously solvented with 20 mL of toluene at room temperature for 3 h. Different concentrations of Na^+–MMT in toluene (1, 2, 5, 8, and 10 wt %) were explored for the intercalation. The resulting SBS/MMT nanocomposites were cast in a self-made vessel, and then, the samples were exposed to radiation from an 80 W/cm medium-pressure mercury lamp in the presence of air at a passing speed of 60 m/min, which corresponded to an exposure duration of 0.1 s per pass. The maximum light intensity at the sample position was measured by radiometry to be 600 mW/cm^2 in the UV range. The resulting SBS/MMT nanocomposites were dried in a vacuum oven at 80°C.

Analytical instruments

FTIR spectroscopy was performed on a WQF-410 FTIR spectrometer (Beijing Second Optical Instruments Factory, China) between 4000 and 400 cm^{-1} in the form of KBr pellets. An ^{1}H-NMR spectrum was collected with an Inova 400 spectrometer (Palo Alto, CA) with $CDCl_3$ as the solvent. The change in the basal spacing of the nanocomposites was measured with an X-ray diffractometer (D8, Bruker, Germany). Cu Kα radiation (λ = 1.54 Å) was used as an X-ray source at a generator voltage of 40 kV and a current of 35 mA. The diffraction angles were scanned from 0.5 to 10° at a rate of 0.2°/min. The d_{001} spacing was calculated on the basis of Bragg's law [$d_{001} = \lambda/(2 \sin \theta)$] at the peak position. The dispersion of the clays in the nanocomposites was further examined with TEM from a JEM-3010 (JEOL, Japan) instrument operating at 80 kV. The sample for TEM analysis was prepared from the central cross section of the extruded pellets normal to the flow direction. Ultrathin sections approximately 50 nm thick were cryocut with a Reichert-Jung Ultracut E microtome and a diamond knife at −50°C. The thermal stability of the samples (ca. 7 mg) was investigated with thermogravimetric analysis (TGA; Netzsch STA 449C) under nitrogen from room temperature (ca. 30°C) to 800°C at a heating rate of 10°C/min. Dynamic mechanical thermal analysis was carried out on a TA Instruments DMTA-V with a tensional module at a frequency of 1 Hz and at a heating rate of 5°C/min from −130 to 110°C. The specimens (size = 1.5 × 6.5 × 50 mm^3) were cut from the center of the samples. The tensile properties of the samples were measured in accordance with ISO 527 at room temperature (ca. 20°C) with a tensile tester (Instron-4302).

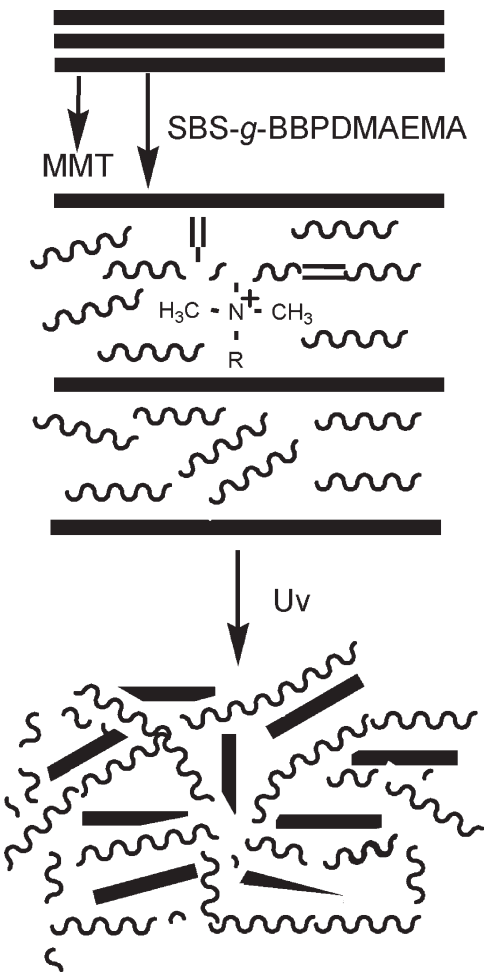

Scheme 2 Scheme for the synthesis of the SBS/MMT nanocomposites.

RESULTS AND DISCUSSION

Characterization of SBS-*g*-4-BBPDMAEMA

The chemical groups of the SBS and SBS-*g*-4-BBPDMAEMA were investigated by FTIR spectra, as shown in Figure 1. The olefinic C—H out-of-plane bending vibration of the *trans*-C=C of the butadiene unit region at 973–945 cm^{-1}, C—H out-of-plane bending vibration of the *cis*-C=C of butadiene at 748 cm^{-1}, and vibration stretching of the =C—H region at 3016–2991 cm^{-1} were clearly observed, and these band intensities were almost the same as those of the pure SBS. Comparing these two IR spectra (Fig. 1), we observed stretching bands at 1730 cm^{-1} for the carbonyl group (—C=O) and carbon–oxygen bond (C—O) at 1235 cm^{-1} in the spectra of SBS-*g*-4-BBPDMAEMA. This suggested that 4-BBPDMAEMA as side chain was successfully grafted onto SBS because the residual 4-BBPDMAEMA and its oligomer were extracted in the Soxhlet extractor with methanol.

To further confirm that 4-BBPDMAEMA was grafted on the backbones of SBS, ^{1}H-NMR was used. The ^{1}H-NMR spectra of pure SBS and SBS-*g*-4-BBPDMAEMA are shown in Figure 2. Compared with the ^{1}H-NMR spectra of pure SBS and SBS-*g*-4-BBPDMAEMA, two new peaks at 3.492 and 2.359 ppm, which were assigned, respectively, to the methyl and methine protons of the grafted point, were observed in SBS-*g*-4-BBPDMAEMA in addition to the expected signals for the block copolymer. The results mean that the monomer 4-BBPDMAEMA was successfully grafted onto SBS.

XRD patterns of the nanocomposites

XRD is usually used to characterize polymer/clay nanocomposites.[41] When the polymer chain intercalates into the interlayer of the clay, the basal spacing of the clay should increase, and the position of the (001) plane peak in the XRD pattern should shift toward a lower angle. Figure 3 shows the XRD patterns of the SBS/MMT. The diffraction pattern of the (001) plane of the raw MMT occurred at 7.08°, and the corresponding distance between the adjacent layers was 1.24 nm. After 5 wt % MMT was added to the SBS matrix, and the position of the (001) plane peak shifted from 7.08° to a lower angle, 5.89°, which corresponded to a basal spacing of 1.50 nm. When the contents of MMT were about 8 and 10 wt %, the position of the (001) plane peaks was at about 5.80° before or after UV exposure. In addition, there was no characteristic peak of MMT in the XRD patterns for the sheets of the SBS/5 wt % MMT

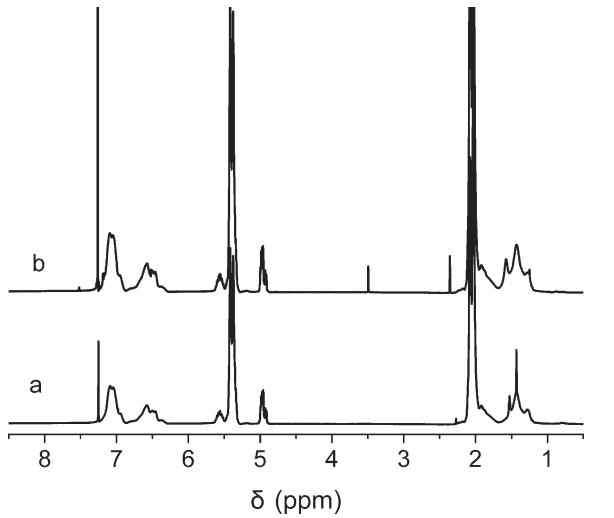

Figure 2 ^{1}H-NMR spectra of the (a) SBS and (b) SBS-*g*-4-BBPDMAEMA.

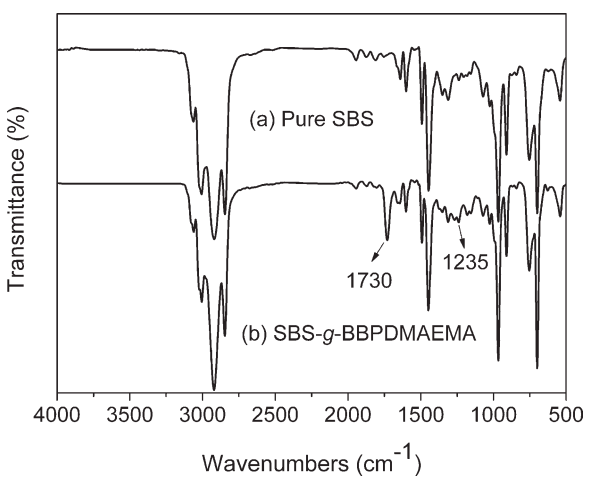

Figure 1 FTIR spectra of the (a) SBS and (b) SBS-*g*-4-BBPDMAEMA.

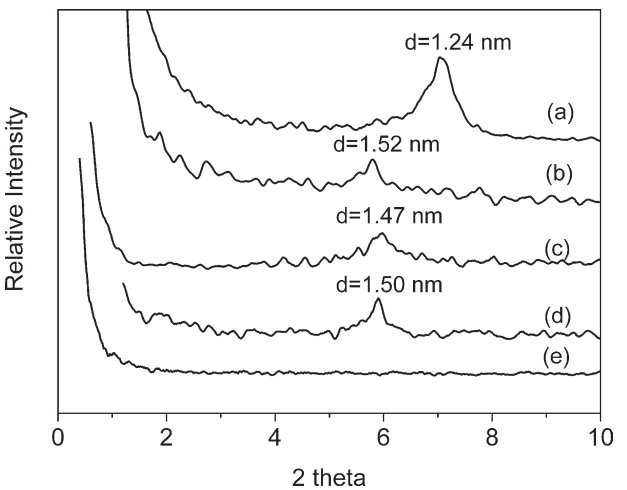

Figure 3 XRD patterns of (a) MMT, (b) SBS/10 wt % MMT with UV exposure, (c) SBS/8 wt % MMT with UV exposure, (d) SBS/5 wt % MMT without UV exposure, and (e) SBS/5 wt % MMT with UV exposure.

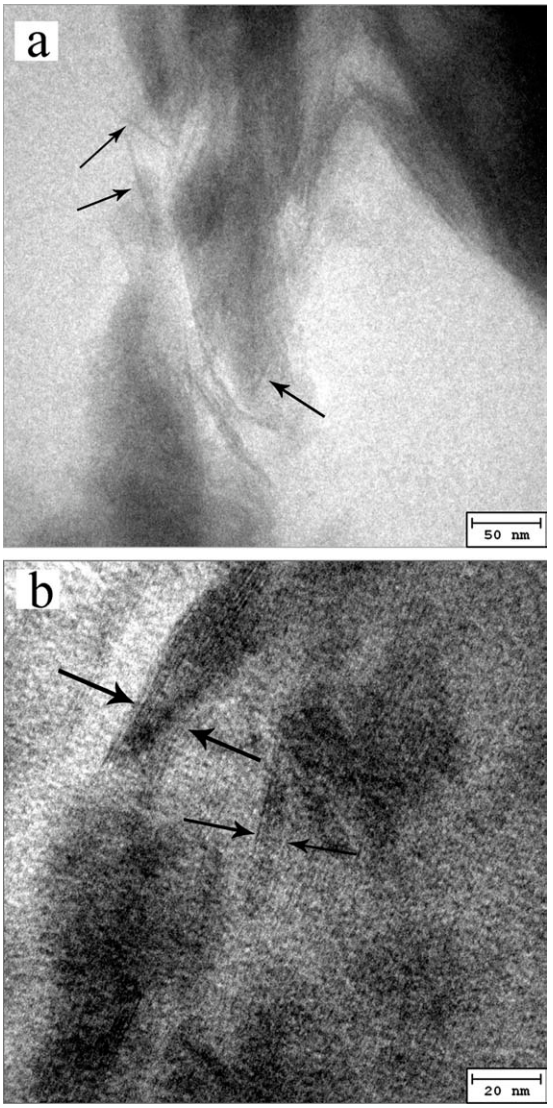

Figure 4 TEM images for SBS/5 wt % MMT with UV exposure.

nanocomposites after UV exposure. This result primarily suggests that the clay platelets should have been exfoliated or completely disordered when the content of MMT was lower than 5 wt % with UV exposure. However, when the content of MMT was greater than 5 wt %, it only obtained an intercalated structure whether it was UV-cured or not. However, the absence of an XRD peak of SBS/5 wt % MMT with UV exposure did not necessarily mean exfoliation, as the observed absence of scattering could be attributed to geometry effects or a lack of sensitivity at the low level of clay loading.

TEM of the nanocomposites

Compared with XRD diffraction patterns, TEM can provide more direct structural information of the nanocomposites. To further investigate the structure of the nanocomposites, TEM images of SBS/5 wt % MMT with UV exposure were taken, and the images are shown in Figure 4. The dark lines and dark and light gray microdomains correspond to the MMT layers and polybutadiene (PB) and PS blocks, respectively. The low-magnification image [Fig. 4(a)] indicated that MMT was mainly desultorily dispersed in the UV-cured polymer. The result means that the galleries of MMT were further expanded or exfoliated after UV exposure. At high magnification, the TEM image [Fig. 4(b)] revealed that MMT was well

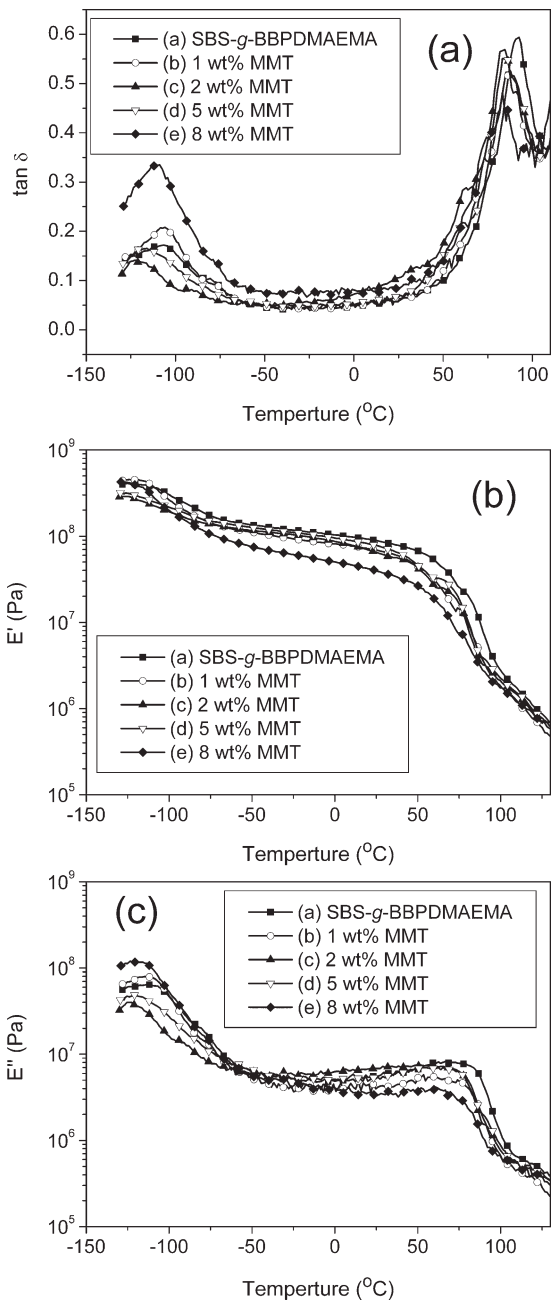

Figure 5 Dynamic mechanical thermal spectra of the SBS-*g*-4-BBPDMAEMA and its nanocomposites: temperature dependence of (a) tan δ, (b) E', and (c) E''.

TABLE I
Thermal Stability of the SBS-*g*-4-BBPDMAEMA and its Nanocomposites

Sample	Onset degradation temperature (°C)[a]	Maximum degradation temperature (°C)	Elastic T_g (°C)	Plastic T_g (°C)
SBS-*g*-4-BBPDMAEMA	368.9	461.2	−105.94	92.51
1 wt % MMT	361.7	461.5	−106.78	87.55
2 wt % MMT	360.0	463.7	−122.53	84.59
5 wt % MMT	372.6	462.3	−115.86	83.22
8 wt % MMT	323.4	462.3	−108.89	83.10

[a] The onset degradation temperature was the temperature of weight lost at 5%.

dispersed in the SBS matrix with an intercalated structure. Therefore, the results of TME indicated that a mixture of partially exfoliated and intercalated structures was present in the nanocomposites.

Dynamic mechanical thermal properties of the SBS-*g*-4-BBPDMAEMA and its nanocomposites

The loss factor (tan δ), E', and E'' versus temperature for the SBS-*g*-4-BBPDMAEMA and its nanocomposites are plotted in Figure 5. As shown in Figure 5(a), in all cases, two T_g values were observed, which showed that the structure of microphase separation was still in existence. The same results were also obtained when Sakurai et al.[42] examined the structure–property relationships of crosslinked SBS using dynamic viscoelastic measurements and tensile stress–strain tests. The lower temperature transition at −110°C was characteristic of the PB domains, whereas the higher temperature transition, at about 90°C, was characteristic of the PS domains. As the content of MMT increased, the value of tan δ relevant to the PB domains decreased to a maximum (−122.53°C with 2 wt % MMT) and then began to increases, whereas the value of tan δ relevant to the PS domains decreased. All of the corresponding data of tan δ are summarized in Table I. These results may have been due to the fact that the MMT platelets were dispersed mainly among the PB block because of they contained lots of quaternary ammonium cations. So, the clay layers had stronger interactions with the PB block and had correspondingly weaker interactions with the PS block, and among the PS block, the MMT platelets could not be intercalated or exfoliated. Thus, the confined PS block was expected to flow, even at temperatures lower than the corresponding T_g of the PS block.

In the E' and E'' curves [Fig. 5(b,c)], variations of E' and E'' as a function of temperature for the SBS-*g*-4-BBPDMAEMA and its nanocomposites with different MMT amounts were clearly observed. Compared with that of SBS-*g*-4-BBPDMAEMA, the E' values of its nanocomposites in the plateau region between the two T_g values decreased a little, and this indicated an increase in the stiffness for the nanocomposites due to the crosslinking structure of the PB domains. In addition, with a continuous increase in content of the MMT, such as for 8% MMT, E' decreased obviously because excessive MMT resulted in phase separation.

Thermal properties of the SBS-*g*-4-BBPDMAEMA and its nanocomposites

The thermal stability of the SBS-*g*-4-BBPDMAEMA and its nanocomposites was evaluated by TGA. The results are presented graphically in Figure 6 and in Table I. The onset degradation temperature of SBS-*g*-4-BBPDMAEMA appeared at 368.9°C. With the increase of the content of MMT from 1 to 8 wt %, the onset degradation temperatures of the nanocomposites decreased, except for 5 wt % MMT. When the content of MMT was increased to 8 wt %, the temperature shifted to a low temperature, which was about 45.5°C lower than that of SBS-*g*-4-BBPDMAEMA. There were two explanations for this phenomenon. The first was that the PB block was crosslinked by UV radiation, so it had relatively more C—C bonds than SBS-*g*-4-BBPDMAEMA, and the bond energy of C—C was 332 kJ/mol, which

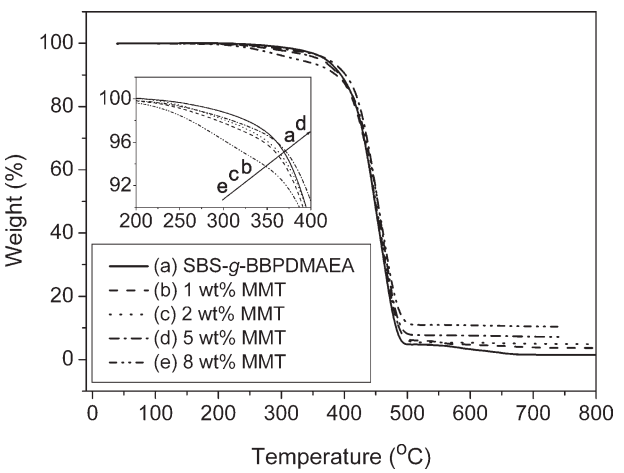

Figure 6 TGA traces obtained from the SBS-*g*-4-BBPDMAEMA and its nanocomposites.

TABLE II
Mechanical Properties of the SBS-*g*-4-BBPDMAEMA and its Nanocomposites

Sample	Tensile strength ± 1 (MPa)	Tensile strength at 300% ± 1 (MPa)	Elongation at break ± 10 (%)
SBS-*g*-4-BBPDMAEMA	21.57	3.24	672.47
1 wt % MMT	13.83	3.65	581.49
2 wt % MMT	13.88	3.71	592.36
5 wt % MMT	17.16	3.75	597.75
8 wt % MMT	11.82	3.47	586.34

was lower than that of C=C (611 kJ/mol). The second reason was that excessive MMT resulted in phase separation. So, the onset degradation temperature of the 8 wt % MMT nanocomposites was lower than that of any of the others.

Mechanical properties of the nanocomposites

The mechanical properties of the nanocomposites were measured and are summarized in Table II. The pure SBS-*g*-4-BBPDMAEMA had a tensile strength of 21.57 MPa and a tensile strength at 300% of 3.24 MPa. The tensile strength of the nanocomposites increased gradually with increasing MMT content before 5 wt % MMT. When 5 wt % MMT was added, the tensile strength of the nanocomposites reached a maximum of about 17.16 MPa; however, with sequential increases in the content of MMT, the tensile strength of the nanocomposites decreased. This may have been due to excessive MMT, which resulted in phase separation. A similar phenomenon is shown in Table II for the elongation at break and tensile strength at 300%. The addition of MMT produced an obvious effect on the elongation, which increased with increasing MMT content and then decreased with sequentially increasing MMT content. These results were in good agreement with those of the dynamic mechanical thermal properties. This indicated that the addition of MMT and UV crosslinking produced significant effects on the tensile strength and elasticity of SBS. The reason may have been that the MMT preferentially dispersed in the PB block of SBS; this led to reduced interaction between PS and PB chains, which moved more easily under tensile force.[43] The mechanism of how the addition of MMT affected the mechanical properties of the nanocomposites needs to be studied further.

CONCLUSIONS

The graft copolymer synthesized from the grafting reaction of SBS with the photoinitiator and quaternary ammonium cations served as an excellent intercalating agent for Na^+–MMT. This synthesized copolymer contained quaternary ammonium cations, which enabled it to ionically exchange with sodium ions in the silicate gallery, and it also contained a photoinitiator and C=C bonds of the SBS, which enabled it to crosslink between the silicate gallery for the preparation of the SBS/MMT nanocomposites via UV exposure. The results of XRD and TEM indicate that a mixture of partially exfoliated and intercalated structures were present in the nanocomposites. In addition, the T_g, thermal stability, and mechanical properties of the SBS-*g*-4-BBPDMAEMA were influenced obviously by the crosslinking and content of MMT.

References

1. Şen, S. Polym Compos 2010, 31, 482.
2. Kickelbick, G. Prog Polym Sci 2003, 28, 83.
3. Castelvetro, V.; De Vita, V. C. Adv Colloid Interface Sci 2004, 108–109, 167.
4. Bourgeat-Lami, E. J Nanosci Nanotechnol 2002, 2, 1.
5. Arroyo, O. H.; Huneault, M. A.; Favis, B. D.; Bureau, M. N. Polym Compos 2010, 31, 114.
6. Kadlecová, Z.; Puffr, R.; Baldrian, J. Eur Polym J 2008, 44, 2798.
7. Usuki, A.; Kojima, Y.; Kawasumi, M.; Okada, A.; Fujushima, A.; Kurauchi, T.; Kamigaito, O. J Mater Res 1993, 8, 1179.
8. Chen, Z.; Gong, K. J Appl Polym Sci 2002, 84, 1499.
9. Lan, T.; Pinnavaia, T. J. Chem Mater 1994, 6, 2216.
10. Giannelis, E. P. Adv Mater 1996, 8, 29.
11. Lee, A.; Lichtenhan, J. D. J Appl Polym Sci 1999, 73, 1993.
12. Liu, T.; Tjiu, W. C.; Tong, Y.; He, C.; Goh, S. S.; Chung, T. S. J Appl Polym Sci 2004, 94, 1236.
13. Park, H.-M.; Liang, X.; Mohanty, A. K.; Misra, M.; Drzal, L. T. Macromolecules 2004, 37, 9076.
14. Dai, X.; Xu, J.; Guo, X.; Lu, Y.; Shen, D.; Zhao, N.; Luo, X.; Zhang, X. Macromolecules 2004, 37, 5615.
15. Weon, J.-I.; Sue, H.-J. Polymer 2005, 46, 6325.
16. Basara, C.; Yilmazer, U.; Bayram, G. J Appl Polym Sci 2005, 98, 1081.
17. Yong, S. L.; Richard, C. L. Biomacromolecules 2006, 7, 2692.
18. Kojima, Y.; Fujushima, A.; Usuki, A.; Okada, A.; Kurauchi, T. J Mater Sci Lett 1993, 12, 889.
19. Messersmith, P. B.; Giannelis, E. P. Chem Mater 1994, 6, 1719.
20. Messersmith, P. B.; Giannelis, E. P. J Polym Sci Part A: Polym Chem 1995, 33, 1047.
21. Xu, R.; Manias, E.; Snyder, A. J.; Runt, J. Macromolecules 2001, 34, 337.
22. Bharadwaj, R. K. Macromolecules 2001, 34, 9189.
23. Hasegawa, N.; Okamoto, H.; Kato, M.; Usuki, A.; Sato, N. Polymer 2003, 44, 2933.
24. Chen, G.-X.; Yoon, J.-S. Polym Degrad Stab 2005, 88, 206.

25. Gilman, J. W.; Kashiwagi, T. SAMPE J 1997, 33(4), 40.
26. Su, S.; Jiang, D. D.; Wilkie, C. A. Polym Degrad Stab 2004, 83, 333.
27. Qin, H.; Zhang, S.; Zhao, C.; Hu, G.; Yang, M. Polymer 2005, 46, 8386.
28. Valera-Zaragoza, M.; Ramírez-Vargas, E.; Medellín-Rodríguez, F. J.; Huerta-Martínez, B. M. Polym Degrad Stab 2006, 91, 1319.
29. Vaia, R. A.; Giannelis, E. P. Macromolecules 1997, 30, 8000.
30. Balazs, A. C.; Singh, C.; Zhulina, E.; Lyatskaya, Y. Acc Chem Res 1999, 32, 651.
31. Balazs, A. C.; Singh, C.; Zhulina, E. Macromolecules 1998, 31, 8370.
32. Groenewold, J.; Fredrickson, G. H. Eur Phys J E 2001, 5, 171.
33. Laus, M.; Francescangeli, O.; Sandrolini, F. J Mater Res 1997, 12, 3134.
34. Chen, Z. H.; Feng, R. C. Polym Compos 2009, 30, 281.
35. Liao, M.; Zhu, J.; Xu, H.; Li, Y.; Shan, W. J Appl Polym Sci 2004, 92, 3430.
36. Zhang, W.; Zeng, J.; Liu, L.; Fang, Y. J Mater Chem 2004, 14, 209.
37. Ha, Y. H.; Kwon, Y.; Breiner, T.; Chan, E. P.; Tzianetopoulou, T.; Cohen, R. E.; Boyce, M. C.; Thomas, E. L. Macromolecules 2005, 38, 5170.
38. Liao, M. Y.; Zhu, J. D.; Xu, H. D.; Li, Y.; Shan, W. J Appl Polym Sci 2004, 92, 3430.
39. Chang, Y. C.; Chou, C. C.; Lin, J. J. Langmuir 2005, 21, 7023.
40. Aalbers, O. Pat. EP 0333, 291 A2 (1989).
41. Xu, H. D.; Li, Y.; Yu, D. S. J Appl Polym Sci 2005, 98, 146.
42. Sakurai, S.; Aida, S.; Nomura, S. Polymer 1999, 40, 2071.
43. Liao, M. Y.; Zhu, J. D.; Xu, H. D.; Li, Y.; Shan, W. J Appl Polym Sci 2004, 92, 3430.